Dual-Polarized Angularly Stable High-Impedance Surface

Seyed Mohammad Hashemi, *Student Member, IEEE*, Sergei A. Tretyakov, *Fellow, IEEE*, Mohammad Soleimani, and Constantin R. Simovski, *Member, IEEE*

***Abstract*—The angular and polarization stability of the effective magnetic wall behavior is critical for successful applications of high-impedance surfaces, especially in low-profile antennas. We suggest an approach to realization of a high-impedance surface with unique magnetic-wall resonance for all incidence angles and for both TE-and TM-polarizations of incident plane waves. In order to achieve this goal we apply the concept of a grounded uniaxial material slab as a realization of a HIS surface and find the effective material parameters required for the unique parallel resonance of the surface impedance. We show that these parameters can be realized with a racemic arrangement of quasi-planar resonant chiral particles. The analytical model of the structure agrees well with full-wave numerical simulations of particular realizations. The maximal deviation of the magnetic-wall resonance frequency in the simulated example is smaller than 0.2% for both polarizations and for the incidence angles varying from 0 to 85 degrees. To our knowledge, this is a qualitatively significant improvement of previously obtained results.**

***Index Terms*—High-impedance surface, grounded uniaxial material slabs, oblique incidence excitation, reflection properties, wide incidence angles.**

I. Introduction

In general, the notion of the surface impedance is applicable to a wide variety of artificial surfaces for electromagnetic applications. Basically any surface with an engineered structure with the period smaller than the wavelength can be characterised in terms of its surface impedance depending on the frequency, plane-wave incidence angle θ and polarization type. Therefore, different types of structures, such as corrugated surfaces [1]–[3], frequency-selective surfaces [4], [5], mushroom structures [6]–[8], etc., can all be categorized as artificial impedance surfaces no matter how different the principles of their operation might seem [9], [10]. In the present paper we concentrate on so-called high-impedance surfaces (HIS) [6]–[10], whose operation implies the magnetic-wall resonance at which the absolute value of their surface impedance significantly exceeds the free space wave impedance.

For most periodic structures their surface impedance Z_s strongly depends on the incidence angle of a plane wave. This angular dependence is different for TE and TM polarized waves (here terms 'TE' and 'TM' as usually mean 'transverse electric' and 'transverse magnetic' with respect to the unit vector normal to the surface). For applications of HIS this dependence is a serious drawback since HIS are mainly used in antenna applications and it is desirable that they mimic the magnetic wall response. If the frequency range of the magnetic wall resonance were unique for the whole spatial spectrum, (including evanescent waves), the radiation field of the horizontal electric dipole located on the HIS would be doubled [6], [9], [10], in accordance to the well-known mirror-image principle. If the magnetic wall is mimicked at the same frequency at least for the whole spectrum of propagating waves, one can expect a significant improvement for the radiation efficiency for low-profile antennas due to the constructive interference of their free-space radiation with the waves reflected by the HIS [8], [10], [11]. However, the actual improvement does not always turn out to be significant. For electrically small antennas, the improvement has even been quoted to be either marginal when it results from the suppression of waves propagating along the substrate in the absence of the HIS [11]–[13] or significant when it results from the formation of the resonant cavity by a finite-size HIS [14], [15]. In both these cases the enhancement of radiation has nothing to do with constructive interaction between the antenna and the HIS. This is rather easy to check through the analysis of the antenna radiation resistance. For majority of known low-profile antennas based on HIS it does not experience the duplication with respect to its value for an antenna located in free space [13]. This is not surprising since the given angular range of the magnetic-wall resonance for most of HIS corresponds only to a relatively small part of the angular spectrum of plane waves excited by the primary source of radiation [10], [16]–[18]. When the incidence angle varies, the resonant frequency of the surface significantly shifts. As a result, the interaction between the antenna and the HIS is a combination of constructive and destructive interference effects [10], [16]–[18].

To design a structure which would mimic the magnetic wall properties for the whole angular spectrum of incident waves becomes an important target. Attempts to improve the angular stability of the magnetic-wall resonance are known [16]–[20], however in these works only a partial stabilization has been achieved (either for small incidence angles [16]–[18] or for one

Manuscript received February 08, 2013; revised April 27, 2013; accepted May 07, 2013. Date of publication June 12, 2013; date of current version July 31, 2013. Part of this work was done during the visit of the first author to Aalto University (Finland), which has been supported in part by the Academy of Finland and Nokia through the center-of-excellence program.

S. M. Hashemi and M. Soleimani are with the Department of Electrical Engineering, Iran University of Science and Technology, Tehran, Iran (e-mail: hashemy@iust.ac.ir; soleimani@iust.ac.ir).

S. A. Tretyakov and C. R. Simovski are with the Department of Radio Science and Engineering/SMARAD CoE, Aalto University, FI-00076 Aalto, Finland (e-mail: sergei.tretyakov@aalto.fi; konstantin.simovski@aalto.fi).

Digital Object Identifier 10.1109/TAP.2013.2263216

polarization [19], [20]—either TE or TM). A quite stable resonance of a HIS for both TE- and TM-waves within the wide range of angles was demonstrated in papers [21], [22], where the special design solution has been suggested based on effective split-rings resonators. In [21], [22] it was shown that the structure possessing a rather angularly stable resonance behaved as a uniaxial magnetic medium with resonant effective permeability. However, papers [21], [22] did not contain a systematic analysis of the angular stability for the magnetic-wall resonance. Moreover, the target of these works was the maximally wide resonance frequency band, whereas the angular stability was only a secondary result.

II. All-Angle and Both Polarizations Grounded Uniaxial Slabs

The present study is based on the idea of artificial uniaxial material layers as promising to design different types of high-impedance surfaces, which was introduced in [23]. In a uniaxial material, the relative permittivity and permeability have different values along the transversal and normal axes (defined with respect to the surface of the material slab). As was shown in [23], the use of uniaxial materials with proper parameters offers a possibility for design of structures with the desired performance of angularly-stable HIS, but some exotic values of the effective material parameters (close to zero or very high) are required. In the following we study one possibility to realize an all-angle and both-polarizations magnetic wall through engineering the needed normal components of the effective permittivity and permeability.

A. Surface Impedance of a Grounded Uniaxial Material Slab

Following [23], here we briefly introduce the general formulas for reflection coefficients from grounded uniaxial slabs and discuss the choice of the required material parameters. In Fig. 1(a), a schematic picture of a grounded uniaxial material slab is shown. The properties of the material slab are described by the effective transverse and normal permittivities (ε_t and ε_n) and permeabilities (μ_t and μ_n), respectively. It is convenient to model the structure shown in Fig. 1(a) with the surface impedance at the top interface of the structure. Assuming only the fundamental-mode plane waves, this surface impedance can be calculated through the transmission-line model [24] (see more details in [25]), illustrated by Fig. 1(b) as the input impedance of a TEM line section of length h. For this we need both the wave impedance Z and the normal component β of the wave number in the uniaxial material of the substrate.

The wave impedances in the uniaxial material read for TE- and TM-polarized incident plane waves, respectively, as [25]

$$Z^{\mathrm{TE}} = j\frac{\omega\mu_t}{\beta_{\mathrm{TE}}} \tag{1}$$

$$Z^{\mathrm{TM}} = j\frac{\beta_{\mathrm{TM}}}{\omega\varepsilon_t}. \tag{2}$$

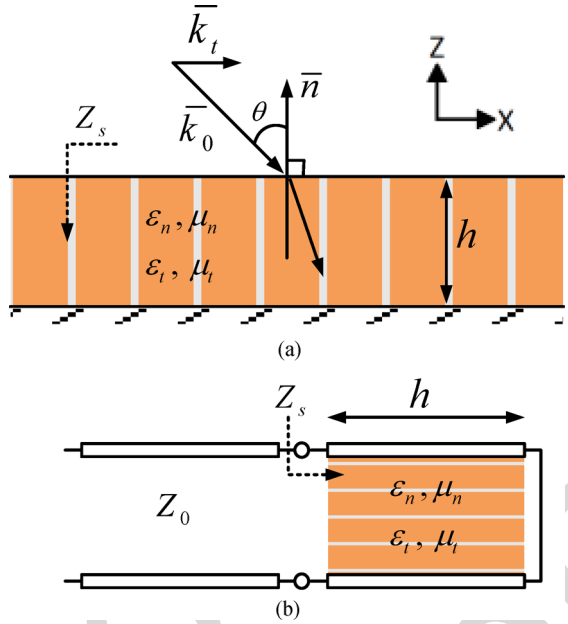

Fig. 1. An illustrative picture of the grounded uniaxial material slab (a). Index t corresponds to the direction tangential to the interfaces, and index n marks the components along the unit vector $\bar{\mathrm{n}}$. Transmission-line model for the grounded uniaxial material slab (b).

Here, the normal components of the wave vectors in the uniaxial slab read [25]

$$\beta^2_{\mathrm{TE}} = \omega^2\varepsilon_t\mu_t - \frac{\mu_t}{\mu_n}k_t^2 \tag{3}$$

$$\beta^2_{\mathrm{TM}} = \omega^2\varepsilon_t\mu_t - \frac{\varepsilon_t}{\varepsilon_n}k_t^2 \tag{4}$$

where $k_t = k_0\sin(\theta)$ is the transverse wave number (θ is the angle of incidence) and k_0 is the wave number in free space. Using the transmission-line model illustrated in Fig. 1(b) and (1)–(4), we can write the surface impedances for both polarizations as

$$Z_s^{\mathrm{TE}} = j\frac{\omega\mu_t}{\beta_{\mathrm{TE}}}\tan(\beta_{\mathrm{TE}}h) \tag{5}$$

$$Z_s^{\mathrm{TM}} = j\frac{\beta_{\mathrm{TM}}}{\omega\varepsilon_t}\tan(\beta_{\mathrm{TM}}h). \tag{6}$$

Let us look more closely into the cases of TM and TE polarizations. Both surface impedances strongly depend on the incidence angle and are different at the same frequency even for the same θ. Our goal for both polarizations is to realize a magnetic conductor whose performance would not be affected by the incident angle nor by the polarizations of the fields.

The plane-wave reflection coefficient R is related to Z_s as [25]

$$R^{\mathrm{TE}} = \frac{Z_s^{\mathrm{TE}} - \eta/\cos(\theta)}{Z_s^{\mathrm{TE}} + \eta/\cos(\theta)} \tag{7}$$

$$R^{\mathrm{TM}} = \frac{Z_s^{\mathrm{TM}} - \eta\cos(\theta)}{Z_s^{\mathrm{TM}} + \eta\cos(\theta)} \tag{8}$$

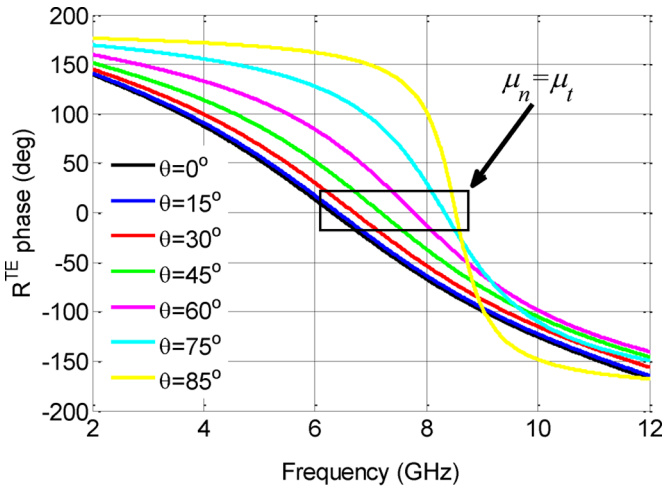

(a)

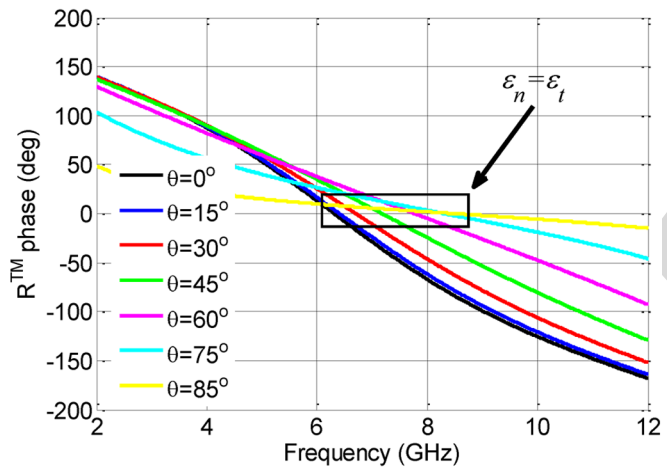

(b)

Fig. 2. Reflection phase of a grounded dielectric slab ($\varepsilon_t = \varepsilon_n = 2.2\varepsilon_0$ and $\mu_t = \mu_n = \mu_0$) with the quarter-wavelength electrical thickness ($\lambda_g/4 = 8$ mm) for the normal incidence and for oblique incidences of 15, 30, 45, 60, 75 and 85 degrees, for (a) TE and (b) TM polarizations.

in the TE and TM-cases, respectively. Here η is the free-space wave impedance. In order to realize a magnetic conductor, the absolute values of the surface impedances for both polarizations need to be maximized. When the surface impedance is infinite, the reflection coefficient R equals $+1$, and the phase of R exactly equals 0. One of the main problems for artificial magnetic conductors is the angular dependencies of the magnetic wall effect. A grounded dielectric slab with the quarter-wavelength electrical thickness serves as a good example here. The magnetic wall effect moves to higher frequencies as the incidence angle grows (see Fig. 2).

B. All-Angle and Both Polarizations Design

In view of possible practical realizations, we select a structure with high values of the normal components of both permittivity and permeability among the possibilities discussed in [23]. The angle-dependence of the normal components of the wave vectors (see (3) and (4)) come from the term $k_t = k_0 \sin(\theta)$. In order to minimize the angular dependency of the normal components of the wave vectors, we should have

$$\mu_n \to \infty, \quad \text{for TE polarization} \tag{9}$$
$$\varepsilon_n \to \infty, \quad \text{for TM polarization.} \tag{10}$$

In this case the normal components of the wave vectors become independent from the incidence angle and equal to each other for both polarizations, since

$$\beta_{\mathrm{TM}}^2 = \beta_{\mathrm{TE}}^2 = \omega^2 \varepsilon_t \mu_t. \tag{11}$$

For this case, we can write the surface impedances (see (5) and (6)) as

$$\begin{aligned} Z_s^{\mathrm{TE}} &= j\frac{\omega\mu_t}{\beta_{\mathrm{TE}}}\tan(\beta_{\mathrm{TE}}h) \\ &= j\frac{\omega\mu_t}{\omega\sqrt{\varepsilon_t\mu_t}}\tan(\beta_{\mathrm{TE}}h) = j\frac{\beta_{\mathrm{TM}}}{\omega\varepsilon_t}\tan(\beta_{\mathrm{TM}}h) = Z_s^{\mathrm{TM}}. \end{aligned} \tag{12}$$

Now both surface impedances do not depend on the incidence angle and are the same for both polarizations ($Z_s^{\mathrm{TE}} = Z_s^{\mathrm{TM}}$). Thus, when the surface impedances for both polarizations are maximized, the magnetic wall effect of the slab becomes independent from the incidence angle for both TM and TE fields.

To illustrate the effectiveness of this method, we assume the Lorentz resonant model for the effective normal permittivities (ε_n) and permeabilities (μ_n) near the resonance frequency (ω_0), given by

$$\varepsilon_n = \varepsilon_h\left(1 + \frac{F_e \times \omega_0^2}{\omega_0^2 - \omega^2 + j\omega_0\Gamma_e}\right) \tag{13}$$
$$\mu_n = \mu_h\left(1 + \frac{F_m \times \omega^2}{\omega_0^2 - \omega^2 + j\omega_0\Gamma_m}\right). \tag{14}$$

Here ε_h and μ_h are the host dielectric slab permittivities and permeabilities, respectively ($\varepsilon_h = \varepsilon_t, \mu_h = \mu_t$). F_e and F_m are constant values, and Γ_e and Γ_m are absorption coefficients. For simplicity of the analytical study we neglect the losses in the structure ($\Gamma_e = \Gamma_m = 0$). The effects of losses is studied at the end of this paper.

For comparison with Fig. 2, a grounded uniaxial material slab example is considered as well. With this example we wish to demonstrate that the normal constitutive parameters of the uniaxial material slab can help us to have incident-angle-insensitive and polarization-independent magnetic wall effect. By substituting (13) and (14) in (3)–(8), for a grounded uniaxial material slab with the quarter-wavelength electrical thickness ($\lambda_g/4 = 8$ mm) and choosing the resonance frequency (ω_0) of the normal components of the constitutive parameters equal to the magnetic wall effect frequency (6.32 GHz), we can see that the zero reflection coefficient phase for both polarizations are stable and the magnetic wall effect of the slab becomes independent from the incidence angle (see Fig. 3). Fig. 3(b) shows some spurious resonances with a very narrow frequency band after the resonance

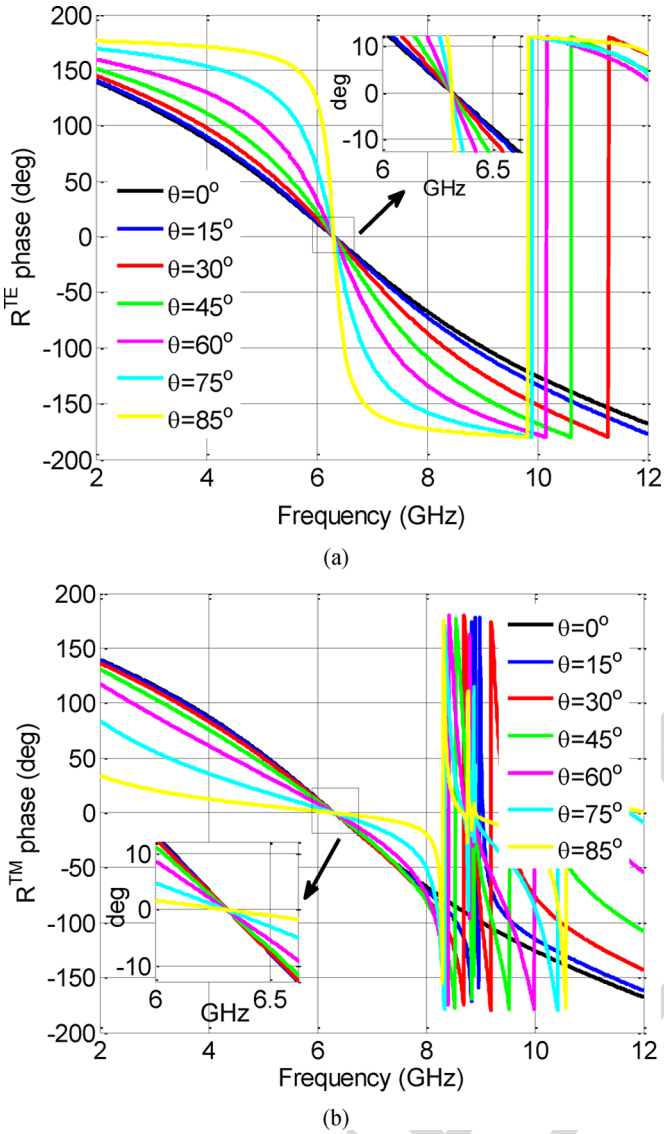

Fig. 3. The simulated reflection phase of grounded uniaxial material slab for the normal incidence and for oblique incidences of 15, 30, 45, 60, 75 and 85 degrees for (a) TE and (b) TM polarizations. The results are calculated using (13), (14). The parameters of the slab are the following: $\varepsilon_t = 2.2\varepsilon_0, \mu_t = \mu_0, h = \lambda_g/4 = 8$ mm, $F_e = F_m = 1, \omega_0 = 6.32$ GHz.

frequency (ω_0) of the normal permittivities. The spurious resonances appear due to the fact that after the resonance frequency $\varepsilon_n \to 0$, at which, according to (4), $\beta_{\mathrm{TM}} \to \infty$.

The above analysis allows us to establish the required condition of grounded uniaxial material slab which will present a unique resonant frequency for all directions of plane-wave incidence: the slab material should have the effective normal permeabilities (μ_n) as described by formulas (9) and the effective normal permittivities (ε_n) as described by formulas (10) for TE and TM, respectively. The effective normal components of the constitutive parameters can be made enough large by introducing a resonance in these parameters. A realization of this condition with proper designed inclusions will be discussed in the following section.

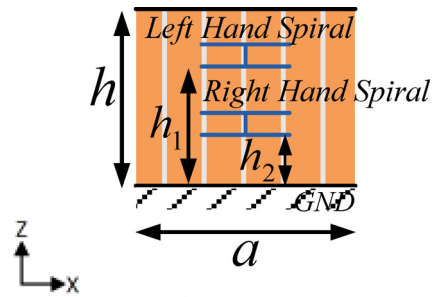

Fig. 4. Proposed rectangular unit cell with racemic arrangement of embedded-circuit inclusions parallel to ground plane.

C. The Proposed Inclusion

The main idea of the design which we introduce here comes from the knowledge that a conducting chiral particle (for example, a metal helix) develops strong electric and magnetic dipole moments at the particle resonance. The resonant frequency for both electric and magnetic polarizabilities is the same, because both moments are created by the same current flowing along the helix. Moreover, the shape of the spiral can be engineered so that the relative effective permittivity and effective permeability of a composite formed by many identical helices are nearly equal to each other. This property was earlier used in the design of matched absorbers and cloaks, where the equality of the permittivity and permeability is an essential requirement [26], [27]. For applications in artificial magnetic walls chirality of the inclusions is not desired (since it produces cross-polarized reflections). Thus, we will use racemic configurations combining particles with the opposite handedness.

Here we propose to use inclusions depicted in Fig. 4, which basically shows (Fig. 5(a)) a broadside-coupled version of the two-turn spiral resonator (2-SR) and other nonbianisotropic topologies. The fundamental magnetic mode of these resonators can be excited by both electric and magnetic fields applied parallel to the ring axis. The susceptibility to the electric field is due to the strong electric field between the upper and lower rings that appear near the resonance. It is well known that the current distribution in a resonator near its resonances does not significantly depend on the exciting field distribution and polarization, and the electric excitation of these resonators excites the fundamental resonant mode (the quasi-static resonance). The electric and magnetic excitations provide effective negative permittivity and permeability, and for avoiding the chirality effect we can use a racemic arrangement of inclusions. In general, these types of resonators can be implemented in two dimensional (2-D) arrays, as an embedded-circuit metamaterial, for providing a uniaxial substrate.

Inspection of the currents at resonances, inferred from the particle symmetries and full-wave electromagnetic simulations, allows us to predict the dipole moments induced in different resonators. The application of an axial, uniform, and time varying electric/magnetic field to the proposed resonators induces current loops at the resonance. Current loops can also be induced by a uniform time varying electric field lying in the particle plane (x-y plane) for broadside coupled spiral resonators (BC-SR)

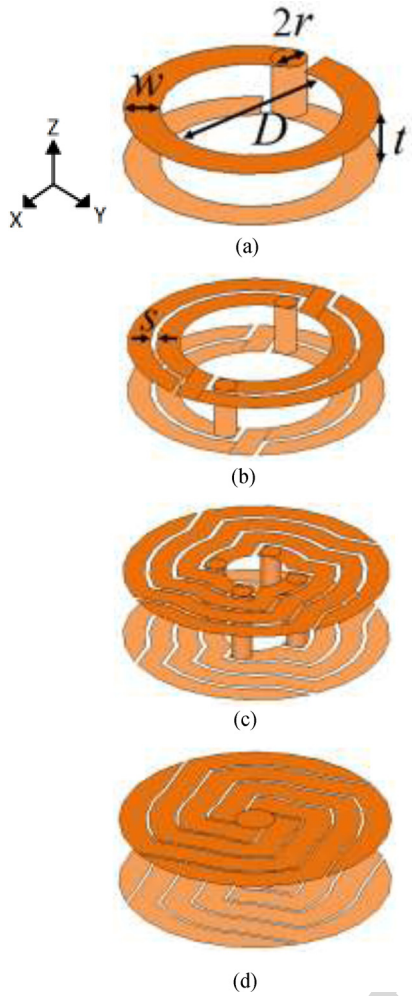

Fig. 5. Topologies for metamaterial resonators with two metal levels (at both sides of a dielectric layer) connected by vias. (a) Broadside coupled spiral resonators (BC-SR). (b) broadside-coupled nonbianisotropic split ring resonator (BC-NB-SRR). (c) Resonant particle with eight appropriately shaped metal elements at both sides of a dielectric layer, connected by four vias. (d) Resonant particle similar to (c) but with one via instead of four vias to simplify fabrication techniques.

(see Fig. 5(a)). This is due to the dipolar electric moment induced in the rings, as a consequence of the cross polarization effects present at the BC-SR first resonance. Similarly, an electric/magnetic field applied in the axial direction is also able to induce this dipolar electric moment. This bianisotropic behavior of BC-SRs is closely related to their topology. Now let us consider a regular planar square array formed by BC-SRs located near an ideally conducting plane and parallel to that plane. As has been shown in [28], there can exist a possibility for a very strong and narrow resonance response from an array of electric dipoles positioned parallel and near to an ideally conducting surface due to very strong interaction between the dipoles array and the ground plane. Thus, the dipolar electric moment induced in the x-y plane should be removed to increase the frequency bandwidth of the magnetic wall effect.

On the basis of the above observations, other resonant particles can be proposed in order to avoid bianisotropy in general. A broadside-coupled nonbianisotropic split ring resonator (BC-NB-SRR) (see Fig. 5(b)) can be proposed in order to avoid the cross-polarization effects and the dipolar electric moment induced in the x-y plane. By combining eight appropriately shaped metal elements at both sides of a dielectric layer and connecting them by four vias, it is possible to design new resonant particles with negligible cross-polarization effects and more complete symmetry in the x-y plane (see Fig. 5(c)). This topology yields more similar response for both TE and TM polarizations. Finally, we can use just one via instead of four vias to simplify fabrication of such inclusions (see Fig. 5(d)).

We realize a periodic racemic arrangement array of embedded-circuit inclusions (depicted in Fig. 5(d)) parallel to ground plane (see Fig. 4) that presents a relatively high artificial normal permittivity (ε_n) and permeability (μ_n) at the frequency of resonance.

III. Numerical Results and Validation

In order to study if the desired response outlined in Section II.B can be indeed realized with the topologies described in Section II.C, we will use the rectangular unit cell depicted in Fig. 4 and verify the response by full-wave simulations using Ansoft's High Frequency Structure Simulator (HFSS). In reference to Fig. 4, "a" is the unit cell size in both x and y-axes directions, "h" is the slab thickness, and "h_1" and "h_2" are the distances to the left- and right-handed inclusions from the ground plane. To have the resonance frequency of the inclusions (responsible for the normal components of the constitutive parameters) equal to the magnetic wall resonant frequency for both TE and TM fields, the inclusions dimensions and the unit cell parameters must be optimized. As an example of the performance of the proposed realization for an all-angle grounded uniaxial material slab, a periodic structure based on the unit cell of Fig. 4 with the following parameters is considered: $t = 1.3$ mm, $w = 0.39$ mm, $s = 0.05$ mm, $2r = 0.58$ mm (in reference to Fig. 5) and $a = 7$ mm, $h = 6.32$ mm, $h_1 = 4.52$ mm and $h_2 = 0.52$ mm and $\varepsilon_t = 2.2\varepsilon_0, \mu_t = \mu_0$, (in reference to Fig. 4).

The phase of the reflection coefficient of the structure (obtained from full-wave electromagnetic simulations by means of the HFSS commercial software) for the normal incidence and for oblique incidences at 15, 30, 45, 60, 75 and 85 degrees for TE and TM polarizations is depicted in Figs. 6(b) and 7(b), respectively. The results of simulations based on the method proposed in Section II.B are also shown in Figs. 6(a) and 7(a) and can be easily compared with the results obtained from the numerical electromagnetic simulation. We assume that the height h is not much smaller than a. In this situation we can neglect higher-order Floquet modes generated by the periodical cells. All parameters are the same as those of Fig. 3 except F_e and F_m values, which are tuned in order to model our example here. In the HFSS simulations, when θ varies from 0° to 85° the zero phase reflection varies between 6.3190 and 6.3204 GHz for TE and between 6.3196 and 6.3316 GHz for TM polarizations. The maximal angular deviation of the resonant frequency is then $\Delta\omega_0/\omega_0 = 0.022\%$ for TE and 0.19% for TM polarization. To avoid cross-polarization effects we have used a racemic arrangement of inclusions in a unit cell. To illustrate the effectiveness of the proposed approach we can check the cross-polarization levels for both TE and TM fields. Full-wave electromagnetic

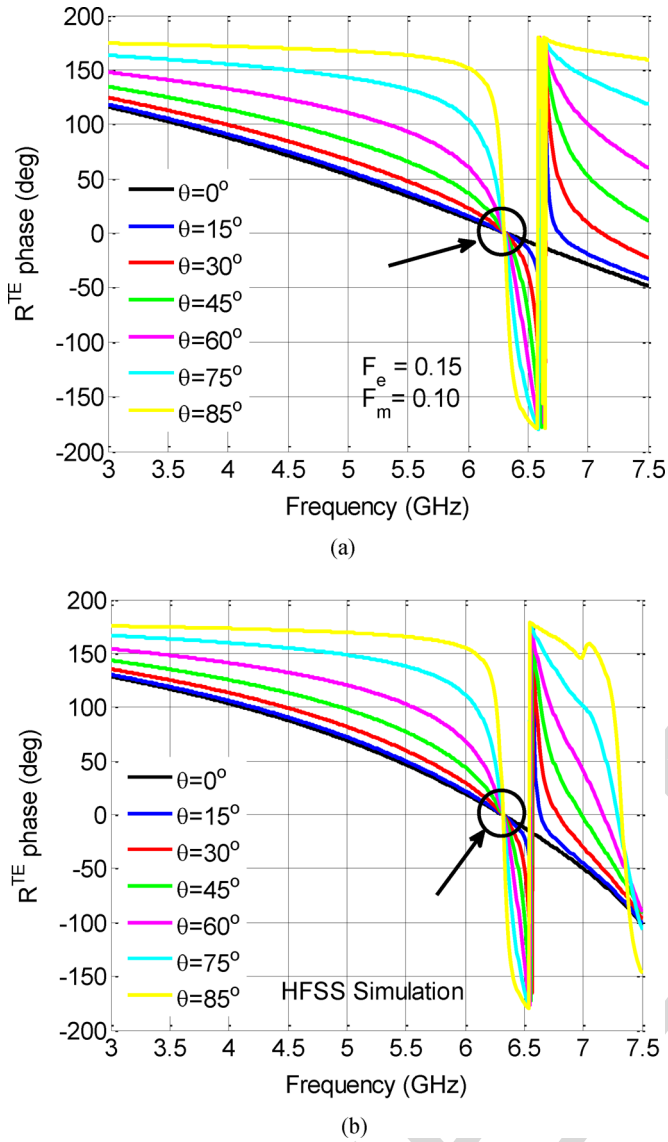

Fig. 6. The reflection coefficient phase of grounded uniaxial material slab for the TE polarization and for the normal incidence, oblique incidences of 15, 30, 45, 60, 75 and 85 degrees. (a) The slab parameters are: $\varepsilon_t = 2.2\varepsilon_0, \mu_t = \mu_0, h = \lambda_g/4 = 8$ mm, $F_e = 0.15, F_m = 0.10, \omega_0 = 6.32$ GHz. The results are calculated using (13), (14). (b) Full-wave electromagnetic simulation of unit cell with parameters: $t = 1.3$ mm, $w = 0.39$ mm, $s = 0.05$ mm, $2r = 0.58$ mm, $a = 7$ mm, $h = 6.32$ mm $= \lambda_g/5.1, h_1 = 4.52$ mm, $h_2 = 0.52$ mm, $\varepsilon_t = 2.2\varepsilon_0$, and $\mu_t = \mu_0$.

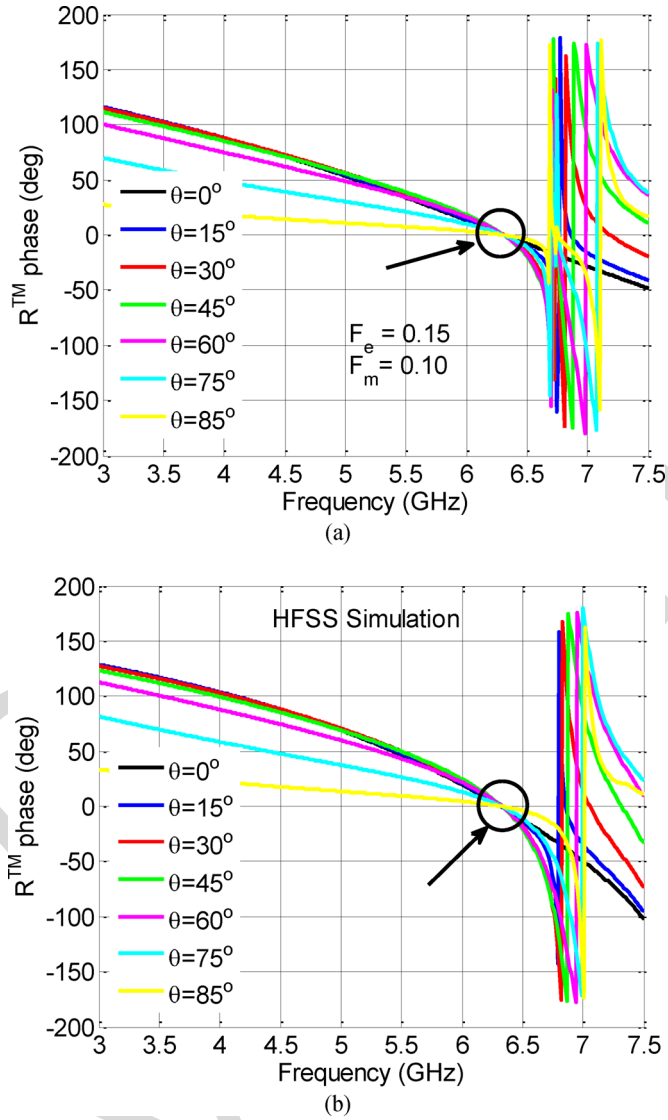

Fig. 7. The reflection coefficient phase of grounded uniaxial material slab for the TM polarization and for the normal incidence, oblique incidences of 15, 30, 45, 60, 75 and 85 degrees. (a) The slab parameters are: $\varepsilon_t = 2.2\varepsilon_0, \mu_t = \mu_0, h = \lambda_g/4 = 8$ mm, $F_e = 0.15, F_m = 0.10, \omega_0 = 6.32$ GHz. The results are calculated using (13), (14). (b) Full-wave electromagnetic simulation of unit cell with parameters: $t = 1.3$ mm, $w = 0.39$ mm, $s = 0.05$ mm, $2r = 0.58$ mm, $a = 7$ mm, $h = 6.32$ mm $= \lambda_g/5.1, h_1 = 4.52$ mm, $h_2 = 0.52$ mm, $\varepsilon_t = 2.2\varepsilon_0$, and $\mu_t = \mu_0$.

simulations show that this value is lower than -22 dB when θ varies from 0° to 85° for both TE and TM polarizations. The frequency bandwidth of HIS is not wide in general and usually it is considered only for the normal incidence. In our case and specially for TE waves, the bandwidth is narrow for large angles of incidence. But other structures (see Fig. 2) without angularly stabilization, completely loose the AMC properties for large incidence angles.

Losses in metamaterials render many applications of such exotic materials less practical. Here we study the effects of losses in our example by considering a particular substrate: Rogers RO5880 with the dielectric constant $\varepsilon_r = 2.2, \tan\delta = 0.0009$ and deposited copper layers of the thickness 35 μm with the bulk conductivity $\sigma = 5.6 \times 10^7$ S/m. When we consider the metal thickness for the resonators, the resonance frequency (ω_0) of the normal components of the constitutive parameters will change. Thus, all the parameters are kept the same as those of Figs. 6 and 7, except the value of h, which is tuned in order to ensure the magnetic wall effect frequency equal to ω_0. The results are depicted in Fig. 8. In the HFSS simulations of the lossy case, when θ varies from 0° to 85°, the zero phase reflection point varies between 6.414 and 6.427 GHz for both TE and TM polarizations. The maximal deviation of the magnetic-wall resonance frequency in this simulated example is again smaller than 0.2% for both polarizations and for the incidence angles varying from

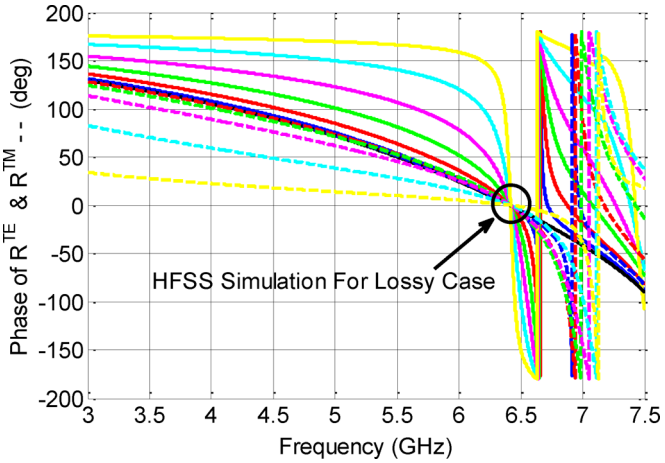

Fig. 8. The reflection coefficient phase of a lossy grounded uniaxial material slab for the TE and TM polarizations. The unit cell parameters are the same as those of Figs. 6 and 7, except $h = 6.22$ mm, $h_1 = 4.42$ mm, $h_2 = 0.42$ mm. The considered substrate is Rogers RO5880 with the dielectric constant $\varepsilon_r = 2.2, \tan\delta = 0.0009$ and the deposited copper layer of the thickness 35 μm with the bulk conductivity $\sigma = 5.6 \times 10^7$ S/m.

0 to 85 degrees. This simulation shows that losses in commercially available substrates do not deteriorate the desired effect and ensures successful realization.

IV. Conclusion

In this work we have suggested and numerically studied a practical implementation of the governing idea of the previous work [23] where the angular stability of a high-impedance surface has been found achievable using a uniaxial magneto-dielectric medium with extreme parameters. We have engineered these parameters designing an effective medium as an array of scatterers which are feasible to manufacture using the existing LTCC technology. A scatterer is formed by two planar metal spirals connected by two vias. The angular stability of the magnetic-wall resonance frequency in our numerical examples is excellent. The shift of the resonance versus the incidence angle is not detectable visually because it is smaller than 1%. This result promises radiation enhancement for low-profile antennas which is related neither to the finite sizes of the HIS nor to the suppression of eigenwaves in the grounded substrate. The gain related to the angularly stable magnetic wall effect can complement these already achieved mechanisms of the antenna radiation enhancement. Experimental realization of the suggested HIS as well as practical designs of low-profile antennas enhanced using our HIS are planned in the future.

References

[1] J. J. Bowman, T. B. A. Senior, P. L. E. Uslenghi, and J. S. Asvestas, *Electromagnetic and Acoustic Scattering by Simple Shapes*. The Netherlands: North-Holland Pub. Co., 1970.

[2] P. S. Kildal, "Artificially soft and hard surfaces in electromagnetics," *IEEE Trans. Antennas Propag.*, vol. 38, pp. 1537–1544, 1990.

[3] S. Maci and P. S. Kildal, "Hard and soft surfaces realized by FSS printed on a grounded dielectric slab," in *Proc. Int. Symp. Antennas Propag. Soc.*, 2004, vol. 1, pp. 285–288, IEEE.

[4] J. C. Vardaxoglou, *Frequency Selective Surfaces: Analysis and Design*. Hertfordshire , U.K.: Research Studies Press, 1997.

[5] B. A. Munk, *Frequency Selective Surfaces: Theory and Design*. New York, NY, USA: Wiley, 2000.

[6] D. Sievenpiper, Z. Lijun, R. F. J. Broas, N. G. Alexopolous, and E. Yablonovitch, "High-impedance electromagnetic surfaces with a forbidden frequency band," *IEEE Trans. Microw. Theory Tech.*, vol. 47, pp. 2059–2074, 1999.

[7] C. Caloz, A. Lai, and T. Itoh, "Wave interactions in a left-handed mushroom structure," in *Proc. Int. Symp. Antennas Propag. Soc.*, 2004, vol. 2, pp. 1403–1406, IEEE.

[8] C. Caloz and T. Itoh, *Electromagnetic Metamaterials: Transmission Line Theory and Microwave Applications*. New York, NY, USA: Wiley, 2005.

[9] D. Sievenpiper, "High-Impedance Electromagnetic Surfaces," Ph.D. dissertation, Univ. California, Los Angeles, CA, USA, 1999.

[10] T. Kamgaing, "High-Impedance Electromagnetic Surfaces for Mitigation of Switching Noise in High-Speed Circuits," Ph.D. Dissertation, Univ. Maryland, College Park, MD, USA, 2003.

[11] S. Clavijo, R. E. Diaz, and W. E. McKinzie, III, "Design methodology for Sievenpiper high-impedance surfaces: An artificial magnetic conductor for positive gain electrically small antennas," *IEEE Trans. Antennas Propag.*, vol. 51, pp. 2678–2690, 2003.

[12] J. R. Sohn, K. Y. Kim, and H.-S. Tae, "Comparative study on various artificial magnetic conductors for low-profile antenna," *Progr. Electromagn. Res.*, vol. PIER-61, pp. 27–37, 2006.

[13] G. Poilasne, "Antennas on high impedance ground planes: On the importance of the antenna isolation," *Progr. Electromagn. Res.*, vol. PIER-41, pp. 237–255, 2003.

[14] A. P. Feresidis, G. Goussetis, W. Shenhong, and J. C. Vardaxoglou, "Artificial magnetic conductor surfaces and their application to low-profile high-gain planar antennas," *IEEE Trans. Antennas Propag.*, vol. 53, pp. 209–215, 2005.

[15] A. P. Feresidis and J. C. Vardaxoglou, "High gain planar antenna using optimised partially reflective surfaces," in *Proc. Int. Symp. Antennas Propag. Soc.*, 2001, vol. 148, pp. 345–350.

[16] A. Monorchio, S. Genovesi, U. Serra, and G. Manara, "Optimal design of artificial magnetic conductors including angular response," in *Proc. Int. Symp. Antennas Propag. Soc.*, 2006, pp. 1931–1934.

[17] F. Bilotti, A. Toscano, L. Vegni, K. Aydin, K. B. Alici, and E. Ozbay, "Equivalent-circuit models for the design of metamaterials based on artificial magnetic inclusions," *IEEE Trans. Microw. Theory Tech.*, vol. 55, pp. 2865–2873, 2007.

[18] C. R. Simovski, P. de Maagt, S. A. Tretyakov, M. Paquay, and A. A. Sochava, "Angular stabilisation of resonant frequency of artificial magnetic conductors for TE-incidence," *Electron. Lett.*, vol. 40, pp. 92–93, 2004.

[19] C. R. Simovski, P. de Maagt, and I. V. Melchakova, "High-impedance surfaces having stable resonance with respect to polarization and incidence angle," *IEEE Trans. Antennas Propag.*, vol. 53, pp. 908–914, 2005.

[20] C. Simovski, T. Rouiller, and I. Melchakova, "Full-angle magnetic conductors and their application in coplanar isolators," in *Proc. 34th Eur. Microwave Conf.*, 2004, pp. 1349–1351.

[21] C. R. Simovski, A. A. Sochava, and S. A. Tretyakov, "New compact and wideband high-impedance surface," in *Antennas and Propagation Society International Symposium, 2004*, 2004, vol. 1, pp. 297–300, IEEE.

[22] C. R. Simovski, M. E. Ermutlu, A. A. Sochava, and S. A. Tretyakov, "Magnetic properties of novel high impedance surfaces," *Microwaves, Antennas & Propagation, IET*, vol. 1, pp. 190–197, 2007.

[23] O. Luukkonen, C. R. Simovski, and S. A. Tretyakov, "Grounded uniaxial material slabs as magnetic conductors," *Progr. Electromagn. Res. B*, vol. 15, pp. 267–283, 2009.

[24] S. A. Tretyakov and C. R. Simovski, "Dynamic model of artificial impedance surfaces," *J. Electromagn. Waves Applic.*, vol. 17, pp. 131–145, 2003.

[25] S. Tretyakov, *Analytical Modeling in Applied Electromagnetics*. Norwood, MA, USA: Artech House, 2003.

[26] E. Saenz, I. Semchenko, S. Khakhomov, K. Guven, R. Gonzalo, E. Ozbay, and S. Tretyakov, "Modeling of spirals with equal dielectric, magnetic and chiral susceptibilities," *Electromagnetics*, vol. 28, pp. 476–493, 2008.

[27] K. Guven, E. Saenz, R. Gonzalo, E. Ozbay, and S. Tretyakov, "Electromagnetic cloaking with canonical spiral inclusions," *New J. of Physics*, vol. 10, no. 11, p. 115037, 2008.

[28] P. A. Belov and S. A. Tretyakov, "Resonant reflection from dipole arrays located very near to conducting planes," *J. Electromagn. Waves Appl.*, vol. 16, pp. 129–143, 2002.

Seyed Mohammad Hashemi (S'08) was born in Tehran, Iran, in 1983. He received the B.Sc. and M.Sc. degrees in electrical engineering from the Iran University of Science and Technology (IUST), Tehran, Iran, in 2006 and 2008, respectively. Since 2008, he has been working toward the Ph.D. degree in electrical engineering at the Iran University of Science and Technology. In October 2012 he joined to the Aalto University, Finland, as a visiting scholar.

His research interests include complex media electromagnetics, optimization methods, antenna and microwave engineering.

Sergei A. Tretyakov (F'09) received the Dipl. Engineer-Physicist, the Candidate of Sciences (Ph.D.), and the Doctor of Sciences degrees all in radiophysics from the St. Petersburg State Technical University, Russia, in 1980, 1987, and 1995, respectively.

From 1980 to 2000 he was with the Radiophysics Department of the St. Petersburg State Technical University. Presently, he is Professor of radio engineering at the Department of Radio Science and Engineering, Aalto University, Finland, and the president of the Virtual Institute for Artificial Electromagnetic Materials and Metamaterials (Metamor-phose VI). His main scientific interests are electromagnetic field theory, complex media electromagnetics and microwave engineering.

Prof. Tretyakov served as Chairman of the St. Petersburg IEEE ED/MTT/AP Chapter from 1995 to 1998.

Mohammad Soleimani received the B.S. degree in electrical engineering from the University of Shiraz, Shiraz, Iran, in 1978 and the M.S. and Ph.D. degrees from Pierre and Marie Curio University, Paris, France, in 1981 and 1983, respectively.

Currently, he is a Professor with the Iran University of Sciences and Technology, Tehran, Iran. He has served in many executive and research positions including: Minister of Information and Communication Technology, Member of Parliament of Iran, Student Deputy of Ministry of Science, Research and Technology, Head of Iran Research Organization for Science and Technology, Head of Center for Advanced Electronics Research Center; His research interests include Electromagnetics, antennas and microwave engineering.

Constantin R. Simovski defended his received the Ph.D. degree in 1986 in the Leningrad Polytechincal Institute, later called St.-Petersburg Polytechnical University, Russia.

In 2000 he defended in the same university the thesis of Doctor of Sciences in physics and mathematics. He has worked in both industry and universtities. Since 2008 he has been with Helsinki University of Technology, now Aalto University, Helsinki, Finland. Current research: new metamaterials for nanosensing, energy harvesting, and nanophotonic components, homogenization and electromagnetic characterization of metamaterials including metasurfaces and high-impedance surfaces.